

MAGNETIC RECONNECTION AND PARTICLE ACCELERATION INITIATED BY FLUX EMERGENCE

Masson, S.¹, Aulanier, G.¹, Pariat, E.^{2,3,4}, Klein, K.-L.¹ and Schrijver, C. J.⁵

Abstract. So as to perform an MHD simulation of the evolution of the corona driven by the evolution of the photosphere, a key aspect is the definition of the boundary conditions for reaching a good compromise between physical conditions and numerical constraints. In this work, we focused on the simulation of a confined flare observed on Nov 16, 2002. As initial configuration, we considered a uniform temperature corona, with a magnetic field resulting from a 3D potential field extrapolation from a SOHO/MDI magnetogram. We prescribed a velocity field at the photospheric boundary of the domain, so as to mimic the observed flow pattern associated to a flux emergence. This resulted in a combination of “slipping reconnection” in a halo of QSLs surrounding a 3D null point, through which a “fan reconnection” regime took place. This simplified approach of flux emergence has successfully reproduced the main characteristics of the observed flare: the flare ribbons observed in the EUV with TRACE being due to the chromospheric impact of particles accelerated along reconnecting field lines, this bimodal regime could explain both the shapes and dynamics of these ribbons. We foresee that this kind of modeling should be able to simulate the evolution of slipping magnetic flux tubes in open configurations, allowing to predict the spatio-temporal evolution of particle beams injected into the heliosphere.

1 Introduction

The emergence of magnetic flux at the photospheric level is partly responsible of the solar activity. Indeed, this process injects magnetic flux and energy in active regions, and it can eventually destabilize the magnetic configuration, resulting in the acceleration of energetic particles through magnetic reconnection. Modeling this process can be done in the framework of MHD. But the photosphere-chromosphere layer displays strong gradients in temperature and density, which involve sharp numerical gradients during any MHD simulation. So the treatment of flux emergence at this interface is not easy to perform, especially when dealing with complex overlaying coronal fields. Coronal simulations, however, in which one simply introduces boundary conditions to reproduce the flux emergence at the photosphere, can be used to simulate the temporal evolution of observed active regions. Here we present the results of a such 3D MHD simulation, directly applied to the interpretation of a solar flare which was driven by flux emergence.

2 Magnetic flux emergence, flare ribbons and coronal magnetic field of the C-class flare

We study a C-class flare which occurred in AR 10191 on Nov 16, 2002. In order to understand its magnetic context, we used SOHO/MDI line-of-sight magnetograms. Figure 1 shows that this region was formed by a negative leading-sunspot, and a positive trailing-sunspot. Within the trailing region, a nearly circular area of negative polarity is enclosed within the dominant positive flux. The flux of this enclosed polarity increased during three days preceding the flare. Between Nov 15 at 12:30 UT and Nov 16 at 06:27 UT, an important flux emergence also occurred in the central region of the AR, between the main polarities (Figure 1, right column).

¹ LESIA, Observatoire de Paris, CNRS, UPMC, Université Denis Diderot, 5 place Jules Janssen, 92190 Meudon Cedex

² Space Weather Laboratory, NASA Goddard Space Flight Center Greenbelt, MD 20771, USA

³ Space Science Division, Naval Research Laboratory, Washington, DC 20375, USA

⁴ CEOSR, George Mason University, Fairfax, VA 22030, USA

⁵ Lockheed Martin Solar and Astrophysics Laboratory, 3251 Hanover Street, Palo Alto, CA 93304-1191, USA

The evolution of the magnetic field essentially produced a diverging migration of opposite polarities, as well as the formation of small bipolar fields, typical of emerging flux events. Since this emergence occurred prior to the flare, one can state that it probably triggered it, according to the standard 2D model (Heyvaerts et al. 1977).

The ribbons of this C-class flare were observed with the TRACE spacecraft in the 1600 Å EUV continuum. Their brightenings are known to be partly produced by the impact in the chromosphere of accelerated particles, travelling along magnetic field lines and originating from the region where they reconnect in the corona (e.g. Mandrini et al. 1991). In the left-bottom panel of Figure 1, the three ribbons of the flare are overlaid upon a co-aligned MDI magnetogram. A circular-ellipsoidal ribbon RC enclosed an elongated ribbon RA, while another elongated ribbon (RB) was located outside of the circular ribbon RC. During the temporal evolution of the flare, these ribbons were progressively formed throughout the extension of the brightenings, which eventually formed a final circular and elongated shape.

The presence of an ellipsoidal ribbon may be a good indicator of the presence of a null point. But only a topological study, using an extrapolation of the magnetic field above the photosphere, could confirm or infirm the existence of such a 3D null point. To perform the extrapolation, as bottom boundary conditions, we used the MDI magnetogram taken on Nov 16 at 06h27 UT, a few hours before the flare took place. We calculated a potential magnetic field (Alissandrakis 1981), since it allowed to obtain a reference field with no free magnetic energy to start with, and preserving the correct magnetic topology. The extrapolation confirmed that a 3D null point was present. It was then shown that it divides the coronal domain in two connectivity domains, separated by a so-called “fan” surface enclosing the included negative polarity. In each domain, a singular spine field line which passes through the null point is also present (see e.g. the Fig. 1 of Pariat et al. 2008). Comparing the positions of the ribbon RC and the magnetic topology, we found that RC is almost perfectly co-spatial with the intersection of the fan surface with the photosphere: they both assumed exactly the same circular-like shape. This perfectly agrees with the flare models which stipulate that ribbons are to be found at the footpoints of the separatrices (e.g. Priest & Forbes 2002). By extension, the ribbons RA and RB respectively correspond to the inner and the outer spines. A key issue is that they are not point-like, as one would assume from the fact that the spine is a single field line.

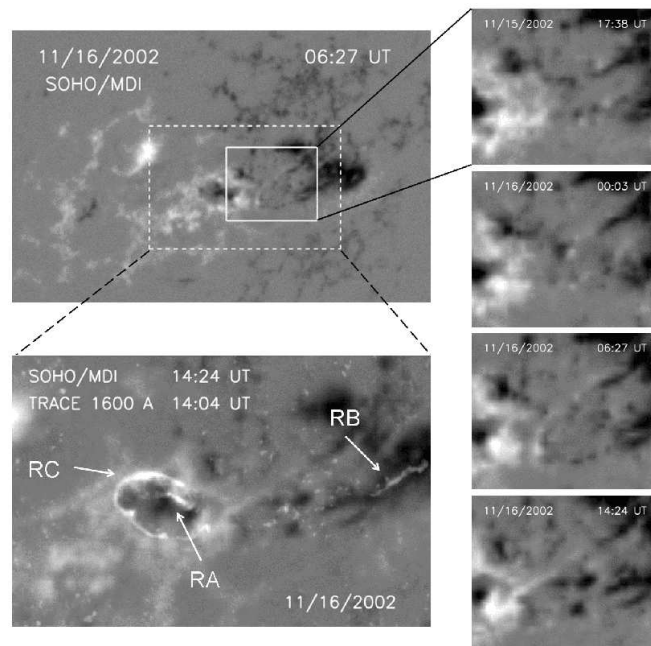


Fig. 1. SoHO/MDI observations of the evolution of AR 10191, beginning 24 hours prior to the flare. Flux emergence is manifested in the white rectangle (right column). The left bottom panel shows the flare ribbon observed by TRACE at 1600 Å overlaid upon the photospheric magnetic field.

3 3D MHD simulation of slipping and fan reconnection & interpretation of the EUV ribbons

To perform an MHD simulation, we used a 3D visco-resistive code which has been developed by Aulanier et al. (2005). This code solves the MHD equations in a cartesian box with a fixed but non-uniform mesh. At the top and side boundaries of the domain, we assumed open conditions. At the bottom boundary, in order to account for the photospheric driving of the corona, we assume line-tied reflective and kinematic conditions. So as to reproduce as reliably as possible the observed evolution of the AR and the flare, we used the output of the potential field extrapolation as an initial condition for the magnetic field. Initially, an uniform density $\rho_{min} = b_{max}^2/\mu c_{A,max}^2 \simeq 5.10^{12} \text{ cm}^{-3}$ was prescribed, and we fixed $c_{A,max} = 1000 \text{ km.s}^{-1}$ as the initial maximum the Alfvén speed. The initial temperature was set to be uniform $T = 3.10^5 \text{ K}$, so that the initial pressure allowed $\beta \ll 1$ everywhere in the domain but close to the null point. The resulting averaged value of $\beta \simeq 10^{-2}$, while $\beta \geq 1$ only within a radius of 1 Mm around the null point. In order to simulate the evolution of the active region, we devised a new method for modeling the observed flux emergence and its coronal consequence in a complex magnetic environment by prescribing a simple analytical diverging velocity field at the bottom boundary (for more details, see Masson et al. 2009). This velocity field was built so as to respect the shape of the emergence region and the velocity ratios and orientations of the flows in this area. But it did not result in the increase of magnetic flux.

Firstly, a thin current sheet developed around the null point, associated with a tearing of the spine, which both induced a fan reconnection regime (according to the terminology of Priest & Titov 1996). Figure 2 shows two snapshots of the reconnecting field lines above the included negative polarity. It appears there clearly that the field lines reconnect at the null point. But before they reconnected at the null point, we found that field lines slipped along the photosphere toward the inner spine, with increasing speed, along a current sheet located inside the included polarity, different from that of the null point. After field lines jumped to the outer spine, they also slipped away from it, with decreasing speed. We found that observed chromospheric ribbons RA and RB did match with the trajectories of the footpoints of these slipping field lines. Also, the temporal evolution of reconnection was consistent with the propagation of brightenings of the ellipsoidal ribbon RC. More details will be given in Masson et al. (2009).

The slipping motion of the field lines before and after the null point reconnection can be explained by the presence of a halo of so-called “Quasi-Separatrix Layers” (QSLs) which surrounds the separatrices, a property that has never been reported before. The presence of QSLs induces slipping and slip-running reconnection (Aulanier et al. 2006) : when field lines reconnect at QSLs, there is not a jump of connectivity, but rather a continuous reconnection pattern along the QSL footprints (Démoulin et al. 1997). This explains why we obtained a slow sub-Alfvénic slipping reconnection regime away from the spine, and a fast super-Alfvénic slip-running reconnection regime close to the spine. Classically, at the null, the field lines jump from one place to another. This bimodal regime naturally explains why the spine-associated flare ribbons are sheet-like instead of point-like.

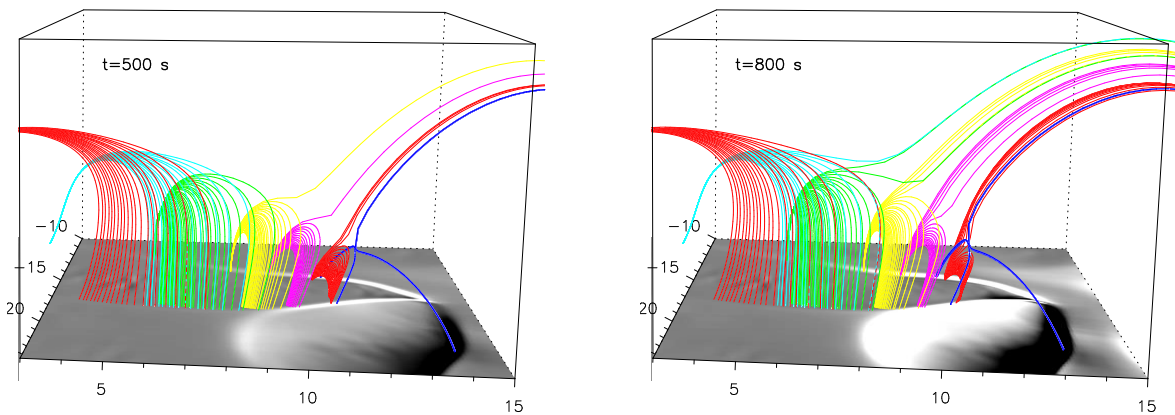


Fig. 2. Evolution of reconnecting magnetic field lines around the null point. The grey scale color coding the electric current density $j_z(z=0)$. Left panel at $t=500 \text{ s}$ and right panel at $t=800 \text{ s}$

4 Extension to open field configurations and SEP beams

The flare-accelerated particles detected at the Earth, are generally coming from active regions that are well-connected to the Interplanetary Magnetic Field (IMF) tube reaching the Earth. Nevertheless, Klein et al. (2008), showed recently that flare-accelerated particles can be detected even if the active region is far from the interplanetary flux tube connecting the Earth, i.e. behind the limb or near the center of the solar disk. They have shown indeed that the open flux tube rooted in the active region can strongly expand in the corona. This magnetic configuration is such that some magnetic field lines of this open flux tube can be connected to the IMF connecting the Earth.

Traditionnaly, if one considers that the reconnection sites are very localized in the active region, and that according to null point reconnection theory, the accelerated particles should mostly propagate along the open outer spine (a single field line). It seems then difficult for flare-accelerated particles to be injected in the part of the extended flux tube connected to the Interplanetary flux tube reaching the Earth. But with the results of the present study, if one considers a magnetic configuration where a null point is included in an halo of QSLs, with an outer spine opened in the corona, one could argue that a slipping motion of the reconnected field lines may take place, exactly like in our closed field configuration of the C-class flare. This type of reconnection regime could successively inject particles in a more or less wide bundle of field lines around the open spine, much like a whip rooted in the low corona swinging in the heliosphere. These effects may explain the injection of particles along the IMF field line connected to earth, even though the latter was not connected to the reconnection point early on. It could also allow particles to be injected in interplanetary flux tubes of different topologies at different times while they slip, thus leading to complex spatio-temporal patterns for particles detected at 1 AU. In the future we plan to conduct this type of analysis, coupling MHD simulations, radio and in-situ observations of particle beams.

5 Conclusion

The analytical diverging velocity field obtained from MDI observations was used as an input in the initial conditions of our MHD simulation. Although this velocity field did not include the increase the magnetic flux, it did reproduce the observed photospheric flows and it allowed for magnetic energy to be stored quasi-statically in the corona. We found a good agreement between the temporal evolution of the magnetic field lines obtained by the simulation and the evolution of the flare ribbons observed by TRACE. Using observational data as initial conditions, our simulation therefore allowed us to interpret the dynamical evolution and the physics of the flare. Our findings, implying the existence of slipping field lines before and after null point reconnection, offer new perspectives for the study of the injection of accelerated particles in the IMF.

References

- Alissandrakis, C. E., 1981, *A&A*, 100, 197
- Aulanier, G., Démoulin, P., Grappin, R., 2005, *A&A*, 430, 1067
- Aulanier, G., Pariat E., Démoulin, P., DeVore, C. R., 2006, *Sol. Phys.*, 238, 347
- Démoulin, P., Bagala, L. G., Mandrini, C. H., Hénoux, M. G., 1997, *A&A*, 325,305
- Heyvaerts, J., Priest, E. R., Rust, D. M., 1977, *ApJ*, 216, 123
- Klein K.-L., Krucker, S., Lointier, G., Kerdraon, A., 2008, *A&A*, 486, 589
- Mandrini, C. H., Demoulin, P., Henoux, J. C., Machado, M. E., 1991, *A&A*, 250,541
- Masson S., Pariat E., Aulanier G., Schrijver C. J., 2009, *ApJ*, in preparation
- Pariat, E., Antiochos, S. K., DeVore, R. C., 2008, *ApJ*, in press
- Priest, E. R., Titov, V. S., 1996, *ApJ*, 472, 840
- Priest, E. R., Forbes, T. G., 2002, *A&A Rev*, 10, 313